ELSEVIER

Chemistry and Physics of Lipids
104 (2000) 23–34

CPL
CHEMISTRY AND PHYSICS OF LIPIDS

www.elsevier.com/locate/chemphyslip

Solid state molecular motion in sucrose octapalmitate as studied by deuterium NMR spectroscopy

G.W. Buchanan [a,*], G. McManus [a], H.C. Jarrell [b]

[a] *Department of Chemistry, Ottawa-Carleton Chemistry Institute, Carleton University, Carleton, Ottawa, Ont., Canada, K1S 5B6*
[b] *Division of Biological Sciences, National Research Council of Canada, Carleton, Ottawa, Ont., Canada, K1A 0R6*

Received 7 April 1999; received in revised form 1 September 1999; accepted 1 September 1999

Abstract

Sucrose octapalmitate-d_{11}, d_{24} and d_{248} have been synthesized. Using ^2H NMR T_1 and analyses of the temperature dependence of the lineshapes, a detailed description of the solid state molecular motional modes is presented. Activation energies for methyl and methylene group rotation in the fatty acyl chains have been determined. The sucrose moiety is found to be static on the solid state deuterium NMR timescale. © 2000 Elsevier Science Ireland Ltd. All rights reserved.

Keywords: Sucrose octapalmitate; Solid state molecular motion; Deuterium NMR spectroscopy

1. Introduction

Lipidic carbohydrate polyesters have been the focus of a broad spectrum of scientific research. Structural variables in these systems are the nature of the esterified fatty acyl chains, the degree of esterification and the type of the carbohydrate moiety. Some of the research interest in these molecules has been based on their properties as bacterial lipopolysaccharide (LPS) endotoxins during bacterial infections (Rietschel et al., 1985; Brandenburg et al., 1993, 1998). Also certain members of this class of molecules function as outer membrane glycolipids (Jarrell et al., 1987; Carrier et al., 1989; Renou et al., 1989) in cells.

The present study examines some members of the class of materials known as sucrose polyesters (SPE). In recent years, extensive research on SPE has led to the discovery of a large range of applications centered around SPE's physicochemical properties (Jandacek and Webb, 1978; Akoh and Swanson, 1989) as they relate to its ability to serve as a lipid-based fat substitute. SPE in the form of a mixture mainly composed of sucrose octaesters with a low amount of sucrose heptaesters of palmitic, stearic, oleic, and linoleic

* Corresponding author. Tel.: +1-613-520-3841; fax: +1-613-520-3749.
E-mail address: gwbuchan@ccs.carleton.ca (G.W. Buchanan)

0009-3084/00/$ - see front matter
PII: S0009-3084(99)00114-0

acids is known as (Olestra*), a low-calorie fat substitute (Akoh, 1995). The ability of SPE to behave as non-caloric lipid-like molecule is due to this high degree of esterification with long chain fatty acids which prevents the hydrolytic action of pancreatic lipase. Thus, esters of this type are not absorbed by the small intestine and pass through the human body unmetabolized (Matteson and Volpenhein, 1972).

With respect to beneficial applications of these systems, it has been demonstrated that SPE is effective as a non-absorbable lipophilic binding agent that can reduce intestinal absorption of certain lipophilic molecules. The presence of SPE as substitute for dietary triacylglycerides has been shown to decrease the absorption of LDL cholesterol (Crouse and Grundy, 1979; Jandacek et al., 1990). Also, SPE has been used to detoxify lipophilic environmental contaminants such as organochlorine pesticides and other halogenated hydrocarbons (Mutter et al., 1988). A more recent application of SPE is as an oral contrast agent for human abdominal MRI studies (Ballinger et al., 1991).

There are, however, some negative aspects of the use of SPE as a non-caloric fat substitute. A source of concern with the use of SPE is that it absorbs the fat-soluble vitamins (Crouse and Grundy, 1979; Mellies et al., 1985), thus depleting the availability of these important micro-nutrients. As a result, food containing SPE must be supplemented with these vitamins (Akoh, 1995). Of further interest is the potential of SPE to interact with and insert into biological membranes. In the latter case, SPE may exhibit similarities to bacterial lipidic carbohydrate polyesters such as lipid A.

In view of the aforementioned importance of SPE, we have begun a study of its interactions with a variety of fat-soluble materials at the molecular level, as well as studies of the insertion of SPE into biological membranes. Initially, however, we are investigating the properties of individual SPE components in order to determine their detailed motional characteristics.

Since a substantial amount of the commercial product Olestra is present as a sucrose octaester of long saturated acyl chains (Jandacek et al., 1990), in the present report we have focused on sucrose octapalmitate (SOP) as a representative compound of SPE. Our hypothesis is that there is likely to be a substantial interaction between the fat-soluble vitamins and SOP in the hydrophobic portion of the molecule — i.e. in the long chain fatty acid region. This should influence dramatically the motional characteristics in these side chains of the SOP system. Since these interactions in vivo are not strictly solution phase ones, we have decided to employ solid phase techniques to examine them. Probably the most powerful method to study motional details of molecules in the solid state is ^{2}H NMR. Accordingly, we have synthesized three different isotopically labeled forms of SOP. In the first compound, all eight palmitoyl chains are perdeuterated, giving rise to SOP-d_{248}. In the second molecule, 11-deuterium atoms are located on the disaccharide rings giving rise to SOP-d_{11}. The third molecule contains all eight palmitoyl methyl groups deuterated, thus producing SOP-d_{24}.

The present work uses ^{2}H solid state NMR T_1 relaxation times and lineshape analysis to probe the dynamics and structural properties of the disaccharide rings and of the saturated fatty acyl chains in polycrystalline SOP. ^{2}H NMR offers two principle advantages for studying molecular dynamics. Firstly, ^{2}H NMR line shapes and relaxation are dominated by the intramolecular quadrupolar interaction. The interpretation of the experimental results is usually not complicated by consideration of other intra or intermolecular spin interactions. Secondly, ^{2}H NMR affords a technique that permits molecular dynamics to be probed over a broad dynamic range (10^0–10^{10} Hz). In order to interpret the experimental data and to correlate them to a molecular motion, a model of the motion must be formulated. The motional model can be built by taking into consideration the possible molecular motions that are consistent with the known molecular structure. Through computer simulations, the analysis of the experimental line shapes for fast and slow motional modes provide insight into detailed aspects of the molecular dynamics.

2. Experimental procedure

2.1. Synthesis of methyl hexadecanoate-d_{31}

Methyl hexadecanoate-d_{31} was synthesized starting with hexadecanoic-d_{31} acid (lot No, A183AP14) purchased from CDN isotopes Ltd. Hexadecanoic-d_{31} acid (2.00 g, 7.38 mmol) was refluxed for 1 h with excess methanol and 1 ml of hydrochloric acid. After cooling to ambient temperature, the product was extracted into dichloromethane (3 × 50 ml). The organic extracts were washed with water followed by a 20% aqueous NaCl solution and then dried over anhydrous sodium sulfate. After filtration, the solvent was removed by rotary evaporation to give crude methyl hexadecanoate-d_{31}. Further solvent removal under vacuum for 1 h gave (1.84 g), 92% yield of the ester which was used without further purification in the next step.

2.2. Synthesis of deuterated sucrose octapalmitate (SOP-d_{248})

This synthesis was based on a procedure developed by Akoh et al. (Akoh, 1990). A 100 ml three-necked round bottom flask equipped with a magnetic stirrer, thermometer, fractional distillation column connected to a condenser, with a vacuum take-off line leading to a liquid nitrogen cold trap, manometer, and a vacuum pump. Methyl hexadecanoate-d_{31} (1.84 g, 6.78 mmol) was added to the reaction flask and flushed with dry N_2 gas for 30 min. Sucrose octaacetate (0.55 g, 0.81 mmol) from Aldrich was added and the system was flushed for an additional 15 min. Sodium metal (0.05 g, 2% of the reactants w/w) was added, the reaction flask was then immersed in a preheated silicon oil bath at 80°C. The reaction mixture was gradually heated to 110°C and vacuum applied to obtain a pressure of about 5 mm Hg. N_2 gas flow was input every 20 min for a 1 min period. The reaction was carried out under these conditions for 2 h at which point heat and pressure were removed. After cooling to room temperature, 1 ml of acetic acid in 100 ml hexane was added to the solution. Subsequent addition of 1 l of methanol caused a precipitate to form and the resulting heterogeneous mixture was stirred overnight. The next day the methanol was removed by gravity filtration. The precipitate was dissolved in a minimum amount of hexane and washed with methanol until the methanol layer was colorless. After drying over anhydrous sodium sulfate and filtration, the hexane was removed from the crude product by rotary evaporation. Subsequent column chromatography (silica gel with hexane:ether:acetic acid (70:30:1) as elution solvent, gave as the first eluted product, sucrose octapalmitate-d_{248} (SOP-d_{248}), 490 mg (24% yield), m.p. 43.8°C from DSC, literature[7] 47–48°C. Thermal decomposition temperature was 300°C from thermal gravimetric analysis.

2.3. Synthesis of sucrose octapalmitate-d_{24} (SOP-d_{24})

SOP-d_{24} was prepared via an identical procedure to that for SOP-d_{248}, except that methylpalmitate-d_3 was employed as a starting material. For SOP-d_{24}, mp is 47–48°C.

2.4. Synthesis of C-deuterated sucrose (Sd_{11})

This synthesis was based on a procedure developed by Koch et al. (Koch and Stuart, 1978) Sucrose (3.0 g, 8.77 mmol) was dissolved in 30 ml of D_2O and rotoevaporated to dryness to give sucrose OD_8. Raney Nickel (20 ml settled volume) was deuterated by exchange by first centrifuging the aqueous metal dispersion and decanting the supernatant H_2O. Subsequently, 10 ml D_2O was added and the solution was vigorously mixed on a vortex followed by centrifugation and decantation of the D_2O. This procedure was repeated three times. D_2O (80 ml) was added to a 250 ml round bottom flask containing 3.0 g dry sucrose-OD_8 and the Raney Nickel. The reaction mixture was refluxed at 100°C for 15 h. After cooling, the reaction mixture was decanted by gravity through a paper filter to remove the Raney Nickel. The solid was washed three times with 40 ml of H_2O and the filtrate was then passed through an Amberite IR-120 cation-exchange resin to eliminate any suspended Raney Nickel. Rotary evaporation was used to remove the aqueous solvent to give

2.62 g (7.39 mmol), 84% yield of a clear syrup of C-deuterated sucrose. The identity of the product was confirmed by ^{1}H NMR spectroscopy.

2.5. Synthesis of C-deuterated sucrose octaactetate (SOAc-d_{11})

C-deuterated sucrose (2.62 g, 7.39 mmol) was dissolved in 50 ml of dry pyridine and 5 ml of acetic anhydride was added. The solution was stirred at room temperature for 11 h. The reaction was quenched by pouring it into ice water (100 ml). Extraction with CH_2Cl_2 (3×50 ml) was carried out, followed by drying over anhydrous sodium sulfate. Solvent removal via rotary evaporation gave 3.7 g of a clear syrup. Thin layer chromatography showed the presence of a mixture of six compounds. This mixture was subjected to column chromatography (silica gel, 130–270 mesh) with 5:1 ether: light petroleum ether as eluant. The fourth eluted product was C-deuterated sucrose octaacetate (300 mg, 0.436 mmol) (59% yield).

2.6. Synthesis of C-deuterated sucrose octapalmitate (SOP-Sd_{11})

C-deuterated sucrose octaactetate (300 mg, 0.436 mmol) was reacted for 2 h with 0.95 g (3.518 mmol) of methylhexadecanoate in the same manner as previously described for the synthesis of SOP-d_{248}. From this reaction, 0.124 g (12.6% yield) of pure SOP-Sd_{11} (mp 46–47°C) was isolated.

2.7. NMR

^{2}H NMR spectra were obtained at 61.1 MHz on a VARIAN Unity 400 NMR spectrometer. Spectra were acquired using the quadrupolar echo sequence as described previously (Fenske et al., 1991) using a $\pi/2$ pulse length of 3.5 μs (5 mm solenoid coil). Samples were enclosed in a glass jacket in which the temperature was regulated to ± 1°C. The recycling delay time was set to be approximately equal to $5T_1$.

2.8. Computer simulations

Simulations were performed on a Silcon Graphics 4D/280S computer using a modified line shape simulation program (Wittebort et al., 1987) based on the general formalism of Torchia and Szabo (Torchia and Szabo, 1982). Simulated line shapes were corrected for the finite width of the experimental 90° pulse in the quadrupolar echo sequence (Bloom et al., 1980). The CD_2 and CD_3 line shapes were simulated separately prior to adding them to each other. In addition to parameters associated with details of the motional model (see below), input parameters for the simulations were as follows: line-broadening 1.5 kHz, half width of plot 2.0×105 kHz, spectrometer frequency 61.1 MHz and pulse interval 35 μs.

3. Results

^{2}H spectra of SOP deuterated in each of the palmitoyl chains are shown as a function of temperature in Fig. 1. At low temperature (135 K) the spectra exhibit two sub-spectral features corresponding to ^{2}H–C bonds associated with static methylene residues with quadrupolar splitting of 126 kHz and to methyl groups undergoing rapid reorientation about their C_3 axis with quadrupolar splitting of 40.1 kHz. As the temperature is elevated both the ^{2}H spectral line shape and integrated intensity changes indicate the onset of chain motion. At 298 K, the spectral lineshape is reminiscent of a motionally averaged quadrupolar interaction characterized by an asymmetry parameter η of approximately 1 and full spectral intensity. The latter suggests that molecular motion is occurring on a timescale that is fast relative to the reciprocal of the residual quadrupolar interaction. At temperatures intermediate between 200 and 298 K, molecular motion is on the timescale of the quadrupolar interaction. Such behavior has been seen previously for structurally related molecules having long polymethylene chains such as phospholipids (Huang et al., 1980; Speyer et al., 1989). In such cases, ^{2}H lineshape changes were consistent with a two-site jump *trans-gauche* isomerization for the methylene

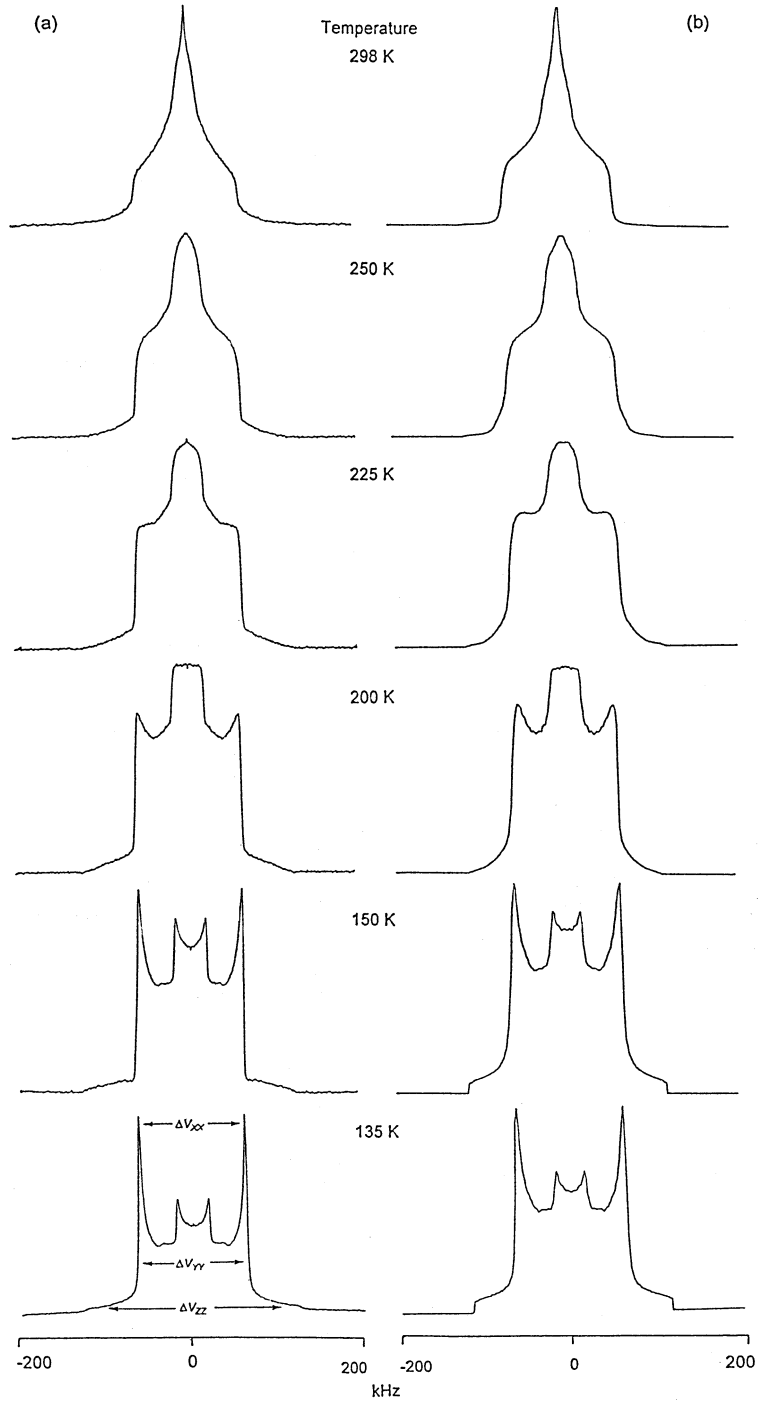

Fig. 1. Experimental (a) and simulated (b) ^{2}H NMR spectra of SOP-d_{248} recorded as a function of temperature. Simulation jump rate and *trans-gauche* population ratio parameters are presented in Table 1, with their respective error values. The spectral singularities ΔV_{ZZ}, ΔV_{YY}, and ΔV_{XX} described in the text are labeled on the bottom right hand side spectrum.

groups. Thus the spectral changes associated with SOP-d_{248} were analyzed in terms of a similar motional model.

3.1. Motional model

Fig. 2 depicts the well known intramolecular *gauche-trans* isomerization of polymethylene chains with the principal axis system of the electric field gradient tensor V_{ZZ}, V_{YY}, and V_{XX} having the polar angles θ and ϕ relative to the static magnetic field (B_0) direction. In the treatment of the *gauche-trans* isomerization model the gauche-(+) and gauche-(−) conformations are considered as having an equal probability of occurrence. Thus, the conformational jump can be taken as a two-site process which known to generate an $\eta = 1$ spectrum with spectral breadth of ca. 120 kHz (Huang et al., 1980; Speyer et al., 1989). For an acyl chain in the all *trans* conformation the principle axis V_{ZZ} is taken to be parallel to the C–D bond and the V_{YY} tensor component is perpendicular to the CD_2 plane and parallel to the axis of molecular motion which is chosen to be the long molecular axis of the acyl chain. In order to define the orientation V_{XX} and V_{YY} the separation between the spectral singularities ΔV_{YY}, ΔV_{XX} and ΔV_{ZZ} were plotted as a function of temperature in Fig. 3. It is quite clear that the ΔV_{YY} singularity for the CD_2 groups remains nearly constant throughout the entire temperature range. This indicates that the V_{YY} tensor must lie parallel with the axis of the molecular motion and perpendicular to the CD_2 bond plane, leaving V_{XX} bisecting the CD_2 bond plane. *Gauche*-(+) or *gauche*-(−) isomerisation around a C–C bond (Fig. 2) displaces the CD_2 by an angle of 120° about the chain long molecular axis. For the CD_3 groups, the ΔV_{YY} singularity shows a similar behavior up to about 217 K. Above this temperature, however, ΔV_{YY} starts to deviate from linearity due to the onset of reorientational motion of the terminal CD_3 groups. To analyze the powder lineshape, spectra spanning the temperature range of 298–135 K were simulated using the model shown in Fig. 2 and a lineshape simulation program developed by Wittebort et al. (Wittebort et al., 1987) based on the general formalism of Torchia and Szabo (Torchia and Szabo, 1982).

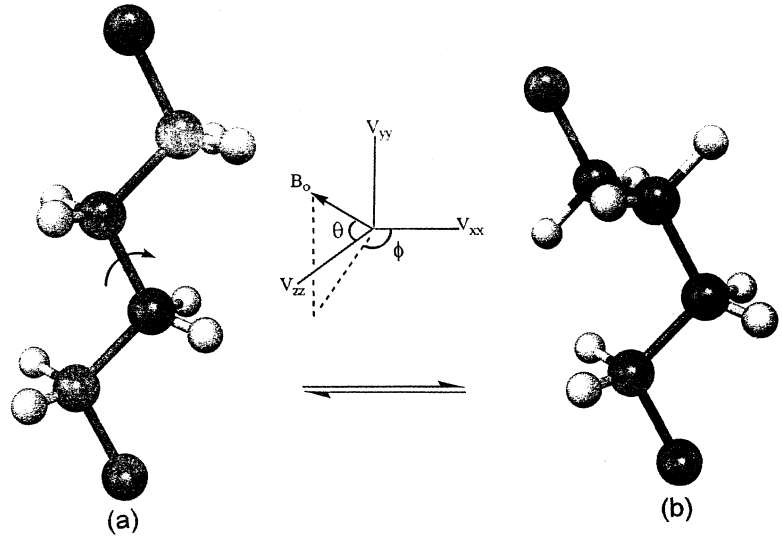

Fig. 2. Model of a twofold jump isomerization in a polymethene chain segment: (a) *trans* conformation; and (b) *gauche* conformation. Also shown are the static magnetic field B_0, and the polar angles θ and ϕ made by the magnetic field vector in the principal axis system of the electric field gradient tensor V_{ZZ}, V_{YY}, and V_{XX}.

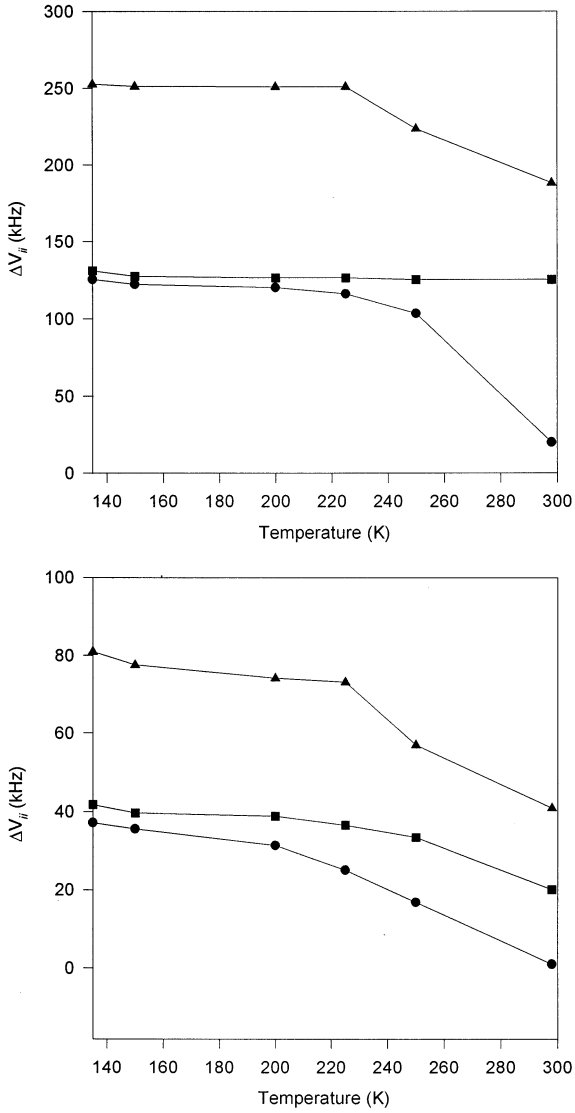

Fig. 3. Plot of the frequency differences, (ΔV_{ii}) between the features of the solid state ^{2}H NMR spectra of Fig. 1a, as a function of temperature. (a) CD_2 and (b) CD_3. (▲, V_{ZZ}; ■, ΔV_{YY}; ●, ΔV_{XX}). Uncertainties for ΔV_{ii} are ± 1 kHz.

3.2. Computer simulation

The powder spectral line shapes for CD_2 and CD_3 were individually simulated as two-site jump exchanges between non-equally populated sites with the C–D bond maintaining the tetrahedral angle over the course of the motion. The methylene groups were simulated using a quadrupolar coupling constant of 171 kHz which described a two site exchange over a tetrahedral geometry. In order to effectively simulate the methyl groups in terms of rates of *trans-gauche* isomerization while accounting for the rapid rotation about a three fold axis and the residual motion present at the chains ends, a variety of quadrupolar coupling constants were used. The results shown in Fig. 1b represent the best fit to the experimental data and were obtained using a quadrupolar coupling constant of 50 kHz instead of the predicted 57 kHz. The lineshape simulated spectra for the methyl and the methylene groups were combined after using a fixed 3:28 deuterium weighting ratio, corresponding to the number of methyl and methylene sites, respectively, throughout the entire temperature range. Inspection of Fig. 1 shows that a simple *trans-gauche* jump motional model adequately reproduces both line shapes and spectral intensity changes at all temperatures. The spectral simulations indicate that varying both the isomerization rate and populations can satisfactorily reproduce the experimental temperature dependent lineshape.

3.3. Analysis of experimental lineshape of the acyl chains

The ^{2}H NMR experimental spectra and computer simulations of SOP-d_{248} as a function of temperature are shown in Fig. 1. The experimental powder line shapes for varying temperatures span the three characteristic ^{2}H NMR motional rates from which structural and motional information can be obtained. The experimental line shape at 298 K is in the fast motion limit where the molecular motion occurs on a timescale much shorter than the reciprocal line width of the static spectrum ($> 10^7$ s^{-1}). The line shape has axial asymmetry ($\eta = 1$) and a spectrum breadth ca 120 kHz suggesting the motional process responsible for the collapse is characteristic of a two site exchange between equally populated sites. As expected at lower temperature, the powder line shape seen at 135 K has axial symmetry ($\eta = 0$) which is consistent with motion occurring on a timescale much longer than the reciprocal line width of the static spectrum ($< 10^{-4}$ s^{-1}). Also

noteworthy, is the reduction of the average quadrupolar splitting of the methyl groups (40.1 kHz) which under rapid rotation about a C_3 axis would be expected to have an average quadrupolar splitting of 42.7 kHz (Batchelder et al., 1983). This discrepancy is consistent with a further motional averaging mechanism operating at the acyl chain ends which has been previously described for various methyl bearing compounds (Batchelder et al., 1983; Taylor et al., 1983) as either a slight departure from the tetrahedral geometry or as the fast torsion fluctuation of the penultimate C–C bond of the $-CD_2CD_3$ groups. Batchelder et al. (Batchelder et al., 1983) have shown that the former and latter description of polycrystalline methyl reorientation could be differentiated by a simple analysis of the observed average quadrupolar splitting as a function of temperature. Inspection of Fig. 3 shows that there is a significant reduction of the values of the observed average quadrupolar splitting as temperature increases indicating that the additional motional averaging mechanism operating at the acyl chain ends is due to large-amplitude asymmetric reorientational motion of the methyl C_3 axis.

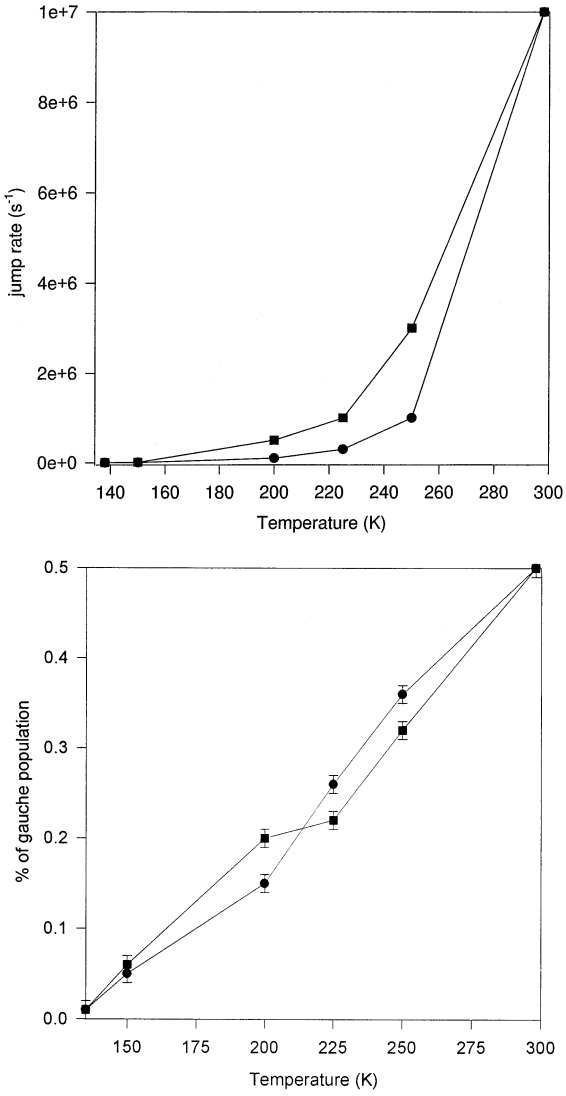

Fig. 4. Comparative representation of Table 1 methylene and methyl group simulation parameters as a function of temperature. (a) Jump rates. (b) *Trans-gauche* isomerization population. Jump rate error values are indicated in Table 1. ●, CD_3; ■, CD_2.

3.4. Analysis of chain end packing

Fig. 4 shows a graphical representation of the simulation values from Table 1 and represents a comparative analysis of CD_2 and CD_3 motion and energetics as a function of temperature. Up to about 217 K, the CD_2 groups have a higher jump rate and *gauche* defect population than do the CD_3. Then above 217 K the situation is reversed. Thus it appears that below 217 K there is insufficient thermal energy to promote large amplitude reorientation of the chain ends. It is to be noted that only by using different jump rates for CD_2 and CD_3 groups as a function of temperature was it possible to simulate the experimentally observed ^2H solid state NMR spectra.

One possible explanation for the decreased degree of motional freedom in the CD_3 groups versus the CD_2 is the existence of intermolecular intercalation in the long chains. This would produce increased steric hindrance, especially at the chain termini, thereby reducing the degrees of motional freedom for the CD_3 moieties. Some X-ray crystallographic evidence for this phenomenon in long chain hydrocarbons has been found (Mnyukh, 1960).

Table 1
Parameters used for the temperature dependent ^2H NMR lineshape simulations of SOP-d_{248} represented in Fig. 1b

Temperature (K)	CD_2 jump rate (s^{-1})	Population *trans*/*gauche*[a]	CD_3 jump rate (s^{-1})	Population *trans*/*gauche*[a]
298	$1.0(\pm 2)\times 10^7$	0.50/0.50	$1.0(\pm 2)\times 107$	0.50/0.50
250	$3.0(\pm 1)\times 10^6$	0.68/0.32	$1.0(\pm 1)\times 106$	0.64/0.36
225	$1.0(\pm 0.5)\times 10^6$	0.78/0.22	$3.0(\pm 0.5)\times 105$	0.74/0.26
200	$5.0(\pm 0.5)\times 10^5$	0.80/0.20	$1.0(\pm 0.5)\times 105$	0.85/0.15
150	$1.0(\pm 1)\times 10^4$	0.94/0.06	$5.0(\pm 1)\times 103$	0.95/0.05
135	$1.0(\pm 2)\times 10^3$	0.99/0.01	$1.0(\pm 2)\times 103$	0.99/0.01

[a] Uncertainties in populations are ± 0.01.

3.5. Sucrose motion

While a *gauche-trans* segmental motion of the acyl chains adequately describes the ^2H lineshapes for SOP-d_{248}, the possibility of other molecular motions must also be considered. Considering the molecular structure similarities of SOP with lipidic molecules, other distinct motional modes could be postulated, namely axial diffusion of the acyl chains, rotation of the entire molecule about an axis or conformational fluctuations of the disaccharide moiety. These motions, occurring either independently or simultaneously, would be observable as a temperature-dependent ^2H NMR lineshape change of SOP-d_{11} where the deuterons are located on the disaccharide moiety. ^2H spectra of SOP-d_{11} were acquired over the same temperature range as was used for SOP-d_{248}. Over the entire temperature range the resulting powder lineshapes did not change and were similar to that shown in Fig. 5 (SOP-d_{11} at 300 K). The quadrupolar splitting of 123 kHz is consistent with a rigid disaccharide moiety with a quadrupolar coupling constant of 164 kHz (Renou et al., 1989). The results confirm the absence of conformational exchange about the glycosidic bond, ring puckering of disaccharide, as well as overall molecular reorientation on a timescale of 10^{-5} s.

3.6. Temperature dependence of T_1

The ^2H spin lattice relaxation times, T_{1z}, at the $\beta = 90°$ spectral singularity associated with the deuteromethyl residues of SOP-d_{24} were measured as a function of temperature using the inversion-recovery technique. The SOP-d_{24} CD_3 powder patterns were found to be identical to the SOP-d_{248} CD_3 group powder patterns measured over the same temperature range. From the simulated jump rates as a function of temperature (Fig. 6a) we have measured the activation energies for the CD_2 and CD_3 motion using the Arrhenius equation. Fig. 6b shows the plot of SOP-d_{24} CD_3 T_{1z} as a function of temperature from which an activation energy was measured using the Arrhenius equation fitted to the high temperature linear part of the curve. Results are shown in Table 2. Activation energies obtained were found to be in good agreement with those reported for *trans–gauche* isomerization or 'kink defect' in solid long chain alkanes (Stohrer and Noack, 1977), and those calculated for fast C_3 axial reorientation of methyl groups in alkanes (Smith and Karplus, 1992). The T_{1z} minimum occurs at 150 K. Using a spectrometer frequency of 61 MHz, this translates into a correlation time of 1.6 ns, a value that is approximately an order of magnitude slower than that found for hydrated phospholipids.

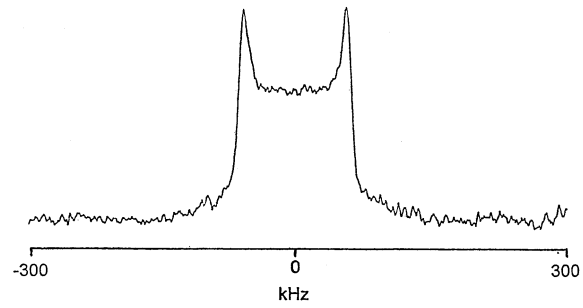

Fig. 5. ^2H solid state NMR of SOP-d_{11} at 300 K. The powder pattern is characteristic of a rigid structure.

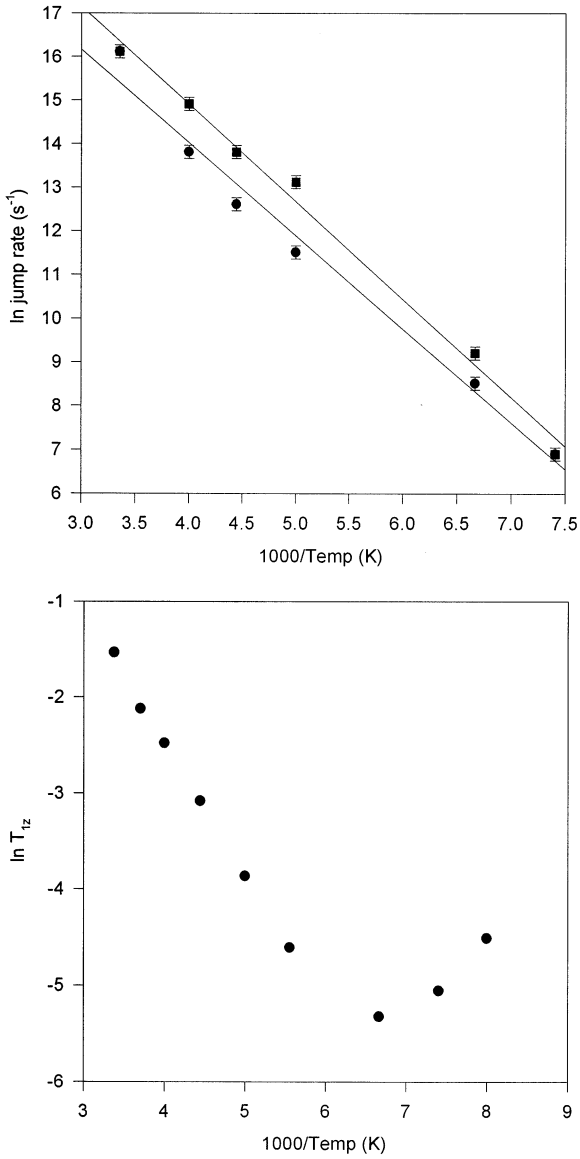

Fig. 6. Representations of Arrhenius plots of (a) the lineshape simulation jump rate values from Table 2 plotted as a function of temperature, (b) Natural logarithm (ln) of SOP-d_{24}, CD_3, T_{1z} plotted as a function of temperature. SOP-d_{24}, CD_3, T_{1z} were measured from $\beta = 90°$ spectral singularities. ●, CD_3; ■, CD_2.

4. Discussion

From our NMR results alone a relatively good description of SOP molecular structure and dynamics can be inferred. However, the comparison with results of structurally related compounds will certainly help assert our proposed molecular structural and dynamics description of SOP.

First, a conformational dynamic representation of the acyl chains can be elaborated on the basis of activation energies. Results show that our experimentally determined activation energy values are in good agreement with activation energies previously found for methylene *trans-gauche* isomerisation and for methyl group reorientation measured for alkanes (Stohrer and Noack, 1977; Smith and Karplus, 1992). This indicates that the motional model described herein can be quite well justified based on the energetics of the system.

Secondly, additional information about the acyl chain motion and packing can be gained through comparison of the literature results on structurally related compounds such as phospholipids (Huang et al., 1980; Speyer et al., 1989), long alkane chains (Mnyukh, 1960; Stohrer and Noack, 1977; Taylor et al., 1983) and triacyglycerol (Jensen and Mabis, 1966). The comparison can be made based on the fact that these compounds have a molecular structural similarity to SOP in that they possess long fatty acyl chains. It was shown through ^2H solid state NMR that for the above mentioned compounds the acyl chain motions could be characterized as ether a *trans-gauche* isomerisation, axial diffusion and or translational motion. The observation of ax-

Table 2
Comparison of experimental and literature values activation energy (E_a) for methylene and methyl groups found in aliphatic alkanes

Molecular motion	E_a, experimental (kJ/mol)	E_a, literature values (kJ/mol)
CD^2 trans-gauche	18.8[a]	20.1 (Stohrer and Noack, 1977)
CD^3 trans-gauche	17.9[a]	
CD^3 reorientation	11.3[b]	12.5 (Smith and Karplus, 1992)

[a] Calculated from jump rates with error of ±15%
[b] Calculated from T_{1z} slope with error of ±10%

ial asymmetry ($\eta = 1$) spectra at 298 K is characteristic of a motional process proceeding with a two-site exchange between equally populated sites with the C–D bond subtending the tetrahedral chain ends (Barnes, 1974; Huang et al., 1980). This effect could be a consequence of having a high degree of order in the packing of the acyl chain generating strong restrictions angle over the course of the motion. Thus, based on the knowledge that axial diffusion and translation motion have more than two-site exchange in their motion it is clear that the only possible motional mechanism operating for the acyl chains of SOP is a *trans-gauche* isomerisation. These observations, combined with the results of the lineshape simulation, provide further evidence of the validity of the proposed *trans-gauche* isomerisation model.

Thirdly, it was shown that the disaccharide moiety is motionless on the NMR time scale and that simulation of the acyl chain CD_2 spectra can be well described by a simple *trans-gauche* jump with a single *trans-gauche* ratio without any axial diffusion of the acyl chain, it would appear that the local acyl chain environment is not significantly perturbing this ratio at each CD_2 site and that there is no large distribution of conformers arising from attachment of the acyl chains to the eight sucrose positions. That is, there does not appear to be a substantial local conformational effect at each site, except for the fast reorientation of the chain ends. This effect could be a consequence of having a high degree of order in the packing of the acyl chain generating strong restrictions on mobility. Such a restriction may be attributed to both inter- and intramolecular interaction between adjacent CD_2 groups. X-ray crystal structure determination of triacylglycerol (Jensen and Mabis, 1966) has shown that similar interactions occur between inter- and intramolecular CD_2 groups due to a close molecular packing of triacylglycerol molecules in which the acyl chains axes are aligned parallel to the long repeat distance of the lattice, extending both above and below, from a perpendicular glycerol backbone. In view of structural and physical similarities of SOP with triacylglycerol it would be reasonable to assume that SOP would have similar molecular packing.

Based on the above discussion we can now elaborate an accurate description of SOP molecular structure in which all eight acyl chains have their long axes closely packed and parallel in both inter- and intramolecular fashions. This packing generates strong motional restriction on the acyl chains which can be described as extending both above and below the plane of a rigid disaccharide unit. This type of molecular structural description was previously implied by X-ray powder diffraction (Jandacek and Webb, 1978) which is now corroborated by our ^2H NMR results. Furthermore, a characterization of SOP dynamics is now available for the acyl chain as well as for the disaccharide unit, which can be used as a template for structural and dynamical analysis of structurally similar molecules, such as for bacterial lipidic carbohydrate polyesters.

5. Conclusions

The present molecular motional model derived from NMR data is the first one available in the literature for solid sucrose octapalmitate. Combined with the previously determined X-ray powder diffraction results (Jandacek and Webb, 1978) a detailed molecular dynamic and structural description of SOP-d_{248} has now been made possible. Future endeavors in this field will involve the study of the influence of various fat soluble compounds (such as Vitamins A and E) on the detailed ^2H NMR lineshapes of the deuterated SOP systems examined in this work.

Acknowledgements

The authors gratefully acknowledge Dr John Katsaras for the gift of methyl deuterated palmitic acid-d_3. G. McManus thanks Dr David J. Siminovitch for several stimulating conversations. G.W. Buchanan gratefully acknowledges continuing financial support from the Natural Sciences and Engineering Research Council of Canada (NSERC).

References

Akoh, C.C., Swanson, B.G., 1989. J. Am. Oil. Chem. Soc. 66, 1581–1587.

Akoh, C.C., Swanson, B.G., 1990. J. Food Sci. 55, 236–243.

Akoh, C.C., 1995. J. Food Sci. 35, 405–430.

Ballinger, R., Malin, R.L., Webb, A.G., 1991. Magn. Reson. Med. 19, 199–202.

Barnes, R.G., 1974. Adv. Nucl. Quadrupole Reson. 1, 335–339.

Batchelder, L.S., Niu, C.H., Torchia, D.A., 1983. J. Am. Chem. Soc. 105, 2228–2231.

Bloom, M., Davis, J.H., Valic, M.I., 1980. Can. J. Phys. 58, 150–157.

Brandenburg, K., Meyer, H.W., Koch, M.H., Weckesser, J., Rietschel, E.T., Seydel, U., 1993. Eur. J. Biochem. 218, 555–563.

Brandenburg, K., Ritcher, W., Koch, M.H., Meyer, H.W., Seydel, U., 1998. Chem. Phys. Lipids. 91, 53–69.

Carrier, D., Giziewicz, J.B., Moir, D., Smith, I.C.P., Jarrell, H.C., 1989. Biochem. Biophys. Acta 983, 100–108.

Crouse, J.R., Grundy, S.M., 1979. Metabolism 28, 994–1000.

Fenske, D.B., Letellier, M., Roy, R., Smith, I.C.P., Jarrell, H.C., 1991. Biochemistry 30, 542–550.

Huang, T.H., Skarjune, R.P., Wittebort, R.J., Griffin, R.G., Oldfield, E., 1980. J. Am. Chem. Soc 102, 7377–7379.

Jandacek, R.J., Webb, M.R., 1978. Chem. Phys. Lipids. 22, 163–176.

Jandacek, R.J., Ramirez, M.M., Crouse, J.R., 1990. Metabolism 39, 848–852.

Jarrell, H.C., Jovall, P.A., Giziewicz, J.B., Turner, L.A., Smith, I.C.P., 1987. Biochemistry 26, 1805–1811.

Jensen, L.H., Mabis, A.J., 1966. Acta Cryst. 21, 770–781.

Koch, H.J., Stuart, R.S., 1978. Carbohydr. Res. 67, 341–348.

Matteson, F.H., Volpenhein, R.A., 1972. J. Lipid. Res. 13, 325–328.

Mellies, M.J., Vitale, C., Jandacek, R.J., Lamkin, G.E., Glueck, C., 1985. J. Am. J. Clin. Nutr. 41, 1–12.

Mnyukh, Y.V., 1960. J. Struct. Chem. (USSR) 1, 346–364.

Mutter, L.C., Blanke, R.V., Jandacek, R.J., Guzelian, P.S., 1988. Toxicol. Appl. Pharmacol. 92, 428–435.

Renou, J.P., Giziewicz, J.B., Smith, I.C.P., Jarrell, H.C., 1989. Biochemistry 28, 1804–1814.

Rietschel, E.T., Brade, L., Kaca, W., Kawahara, K., Lindner, B., Luderitz, T., Tomita, T., Schade, U., Seydel, U., 1985. Prog. Clin. Biol. Res. 189, 31–51.

Smith, J.C., Karplus, M., 1992. J. Am. Chem. Soc. 114, 801–812.

Speyer, J.B., Weber, R.T., Das Gupta, S.K., Griffin, R.G., 1989. Biochemistry 28, 9569–9574.

Stohrer, M., Noack, M., 1977. J. Chem. Phys. 67, 3729–3738.

Taylor, M.G., Kelusky, E.C., Smith, I.C.P., 1983. J. Chem. Phy. 78, 5108–5112.

Torchia, D.A., Szabo, A., 1982. J. Magn. Reson. 49, 107–121.

Wittebort, R.J., Olejniczak, E.T., Griffin, R.G., 1987. J. Chem. Phys. 86, 5411–5420.